EPJ manuscript No.
(will be inserted by the editor)

High-precision mass measurements of ^{25}Al and ^{30}P at JYFLTRAP

L. Canete, A. Kankainen, T. Eronen, D. Gorelov, J. Hakala, A. Jokinen, V.S. Kolhinen, J. Koponen, I.D. Moore, J. Reinikainen, and S. Rinta-Antila

University of Jyvaskyla, P.O. Box 35 (YFL), FI-40014 University of Jyvaskyla, Finland

Received: date / Revised version: date

Abstract. The masses of the astrophysically relevant nuclei ^{25}Al and ^{30}P have been measured with a Penning trap for the first time. The mass-excess values for ^{25}Al ($\Delta = -8915.962(63)$ keV) and ^{30}P ($\Delta = -20200.854(64)$ keV) obtained with the JYFLTRAP double Penning trap mass spectrometer are in good agreement with the Atomic Mass Evaluation 2012 values but ≈5-10 times more precise. A high precision is required for calculating resonant proton-capture rates of astrophysically important reactions ^{25}Al$(p,\gamma)^{26}$Si and ^{30}P$(p,\gamma)^{31}$S. In this work, $Q_{(p,\gamma)} = 5513.99(13)$ keV and $Q_{(p,\gamma)} = 6130.64(24)$ keV were obtained for ^{25}Al and ^{30}P, respectively. The effect of the more precise values on the resonant proton-capture rates has been studied. In addition to nuclear astrophysics, the measured Q_{EC} value of ^{25}Al, 4276.805(45) keV, is relevant for studies of $T = 1/2$ mirror beta decays which have potential to be used to test the Conserved Vector Current hypothesis.

PACS. 21.10.Dr Binding energies and masses – 26.30.Ca Explosive burning in accreting binary systems (novae, x-ray bursts) – 27.30.+t $20 \leq A \leq 38$

1 Introduction

Classical novae are frequent and bright phenomena occurring when a white dwarf accretes hydrogen-rich material from its companion star [1,2]. This leads to a thermonuclear runaway which is observed as a sudden increase in the star's luminosity. Novae reach peak temperatures up to ≈0.4 GK which limits the nucleosynthesis to nuclei with masses below $A \approx 40$. Detailed reaction network calculations have been carried out for nova nucleosynthesis (see *e.g.* Refs. [3–5]). As the light nuclei close to the $N = Z$ line have become more and more accessible experimentally, the calculations start to have a solid experimental foundation offering a unique possibility to compare with observations. In this work, we have studied nuclei relevant for nova nucleosynthesis, ^{25}Al and ^{30}P.

Novae have been proposed to contribute to the amount of cosmic, 1809-keV beta-delayed γ-rays of ^{26}Al [6,7] which gave the first evidence for ongoing nucleosynthesis in the interstellar medium [8]. More recent observations with the COMPTEL telescope on CGRO [9] and SPI on INTEGRAL [10] have shown that the ^{26}Al distribution in the Galaxy is irregular with some localized regions extended over the entire plane of the Galaxy, thus pointing towards massive stars and their supernovae as a source for galactic ^{26}Al γ-rays [10–12]. The nova contribution to the galactic ^{26}Al has a smoother distribution and is estimated to be less than 0.4 solar masses [6] compared to 2.8(8) solar masses determined from SPI/INTEGRAL data [10]. However, this contribution has to be taken into account *e.g.* when estimating the distribution and frequency of core-collapse supernovae in the Galaxy from the amount of cosmic 1809-keV γ-rays.

The production of the ground state of ^{26}Al can be bypassed in novae and other astrophysical scenarios via a reaction sequence leading to the shorter-lived isomeric state of ^{26}Al: ^{25}Al$(p,\gamma)^{26}$Si$(\beta^+)^{26}$Al^m. The isomeric state ^{26}Al^m decays via superallowed beta decay to the ground state of ^{26}Mg, and thus does not contribute to the amount of galactic 1809-keV γ-rays. The proton-capture rate for ^{25}Al$(p,\gamma)^{26}$Si has a direct effect on the production of ^{26}Al: the more likely it is to proceed via proton captures than via the sequence ^{25}Al$(\beta^+)^{25}$Mg$(p,\gamma)^{26}$Al, the fewer 1809-keV γ-rays will be produced. The Q value for the ^{25}Al$(p,\gamma)^{26}$Si reaction is essential as the reaction rates for the proton captures as well as for the inverse photodisintegration reactions depend exponentially on it. Since the mass of ^{26}Si has already been determined with a high precision at JYFLTRAP [13], the mass of ^{25}Al remains the limiting factor for the precision of the Q value.

About one third of novae have an underlying white dwarf containing oxygen, neon and magnesium. These ONe novae reach higher peak temperatures and can synthesize heavier elements than classical carbon-oxygen novae [14]. There, the reaction ^{30}P$(p,\gamma)^{31}$S acts as a gateaway towards heavier elements since the beta-decay half-life of ^{30}P is long (≈2.5 min) compared to typical novae timescales. The alternative route via ^{30}S$(p,\gamma)^{31}$Cl is hindered by inverse photodisintegration reactions on ^{31}Cl. José *et al.* [15] have shown that changing the ^{30}P$(p,\gamma)^{31}$S rate has a dramatic effect on the abundance of ^{30}Si produced via β^+ de-

cay of ^{30}P. The abundance of ^{30}Si is important for assigning presolar grains as being of nova origin [16,17]. These grains have higher than average ^{30}Si/^{28}Si and close to solar ^{29}Si/^{28}Si abundance ratios. Therefore, a more accurate knowledge on the ^{30}P$(p,\gamma)^{31}$S reaction is needed for calculating abundance ratios for different nova environments, to increase our knowledge of novae and underlying white dwarfs in general. The reaction rate depends exponentially on the proton-capture Q value for which the mass of ^{31}S is already well known [18], thus the mass of ^{30}P is the limiting factor in the precision.

In this paper, we have determined the masses of ^{25}Al and ^{30}P with a Penning trap for the first time. The current mass values in the Atomic Mass Evaluation 2012 (AME12) [19] are mainly based on old (p,γ) experiments on ^{24}Mg and ^{29}Si, respectively. The described experiment was also the first on-line mass measurement of neutron-deficient nuclei at the new Ion Guide Isotope Separator On-Line facility, IGISOL-4, at the University of Jyväskylä [20,21]. The 7-T superconducting solenoid housing the JYFLTRAP double Penning trap spectrometer [22] had to be re-energized at IGISOL-4. Therefore, we have also carried out a new measurement of temporal fluctuations of the magnetic field strength in this work.

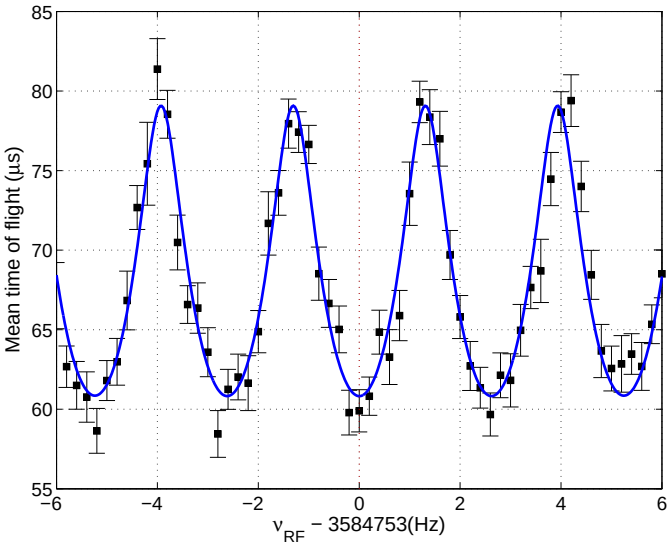

Fig. 1. A Ramsey time-of-flight ion-cyclotron resonance for ^{30}P obtained with an excitation pattern of 25 ms (On) - 350 ms (Off) - 25 ms (On). The number of ions per bunch has been limited to 1-2 ions per bunch and the total number of ions to obtain this spectrum is 1203. The black squares with uncertainties are the average TOF, and the solid (blue) line is the fitted line shape.

2 Experimental method

The IGISOL-4 facility at the Accelerator Laboratory of the University of Jyväskylä was employed in combination with the JYFLTRAP double Penning trap mass spectrometer [22] for the mass measurements of ^{25}Al and ^{30}P. A beam of 40-MeV protons from the K-130 cyclotron impinged into a thin, few mg/cm^2-thick Si or ZnS target at the entrance of the IGISOL gas cell. The fusion-evaporation reaction products were stopped in helium gas and extracted with the help of a sextupole ion guide (SPIG) [23]. The continuous beam was accelerated to 30 keV and the mass number A was selected using a 55° dipole magnet with a mass resolving power ($M/\Delta M$) of ≈500. The mass-separated beam was further sent into a radio frequency quadrupole cooler and buncher (RFQ) [24] which decelerates and cools the ions and releases them into JYFLTRAP as short bunches. JYFLTRAP mass spectrometer consists of two Penning traps, the purification trap, which is used for isobaric purification of the beam via the mass-selective buffer gas cooling-technique [25], and the precision trap, which is used for precision mass measurements.

The time-of-flight ion-cyclotron resonance method (TOF-ICR) [26,27] was utilized for the mass measurements. Once the ions were injected into the precision trap, a short magnetron excitation ν_- was applied followed by a quadrupolar excitation. The frequency of the quadrupolar excitation was scanned around the cyclotron frequency ν_c:

$$\nu_c = \nu_+ + \nu_-, \tag{1}$$

where ν_+ is the reduced cyclotron frequency and ν_- the magnetron frequency of the ion. The motion of the ions in the resonance is fully converted from magnetron to cyclotron within the excitation time if the amplitude has been chosen correctly. As a result, the ions in resonance in the strong magnetic field gradient undergo a stronger axial force. Therefore, they have a shorter time of flight from the Penning trap to a micro-channel plate detector (MCP). In this experiment, we used time-separated oscillatory fields for the quadrupolar excitation (Ramsey method) in the precision trap [28–30]. The quadrupolar excitation was applied as two 25-ms fringes separated by 150 ms for ^{25}Al and by 350 ms for ^{30}P. A typical TOF-ICR obtained for ^{30}P is shown in Fig. 1.

The mass of the ion m_{ion} depends on the measured cyclotron resonance frequency via Eq. 2:

$$\nu_c = \frac{1}{2\pi} \times \frac{qB}{m_{ion}}, \tag{2}$$

where q denotes the charge of the ion and B is the magnetic field strength in the trap. The magnetic field is regularly determined via similar measurements with a reference ion whose atomic mass m_{ref} is already precisely known, and linearly interpolating the cyclotron resonance frequency $\nu_{c,ref}$ to the time of the measurement of the ion of interest. The measured frequencies were corrected for the count-rate effect [31] whenever possible. The atomic mass m for the isotope of interest is then determined via:

$$m = r(m_{ref} - m_e) + m_e, \tag{3}$$

where $r = \nu_{c,ref}/\nu_c$ is the frequency ratio between the reference ion and the ion of interest, and m_e is the electron mass. The differences in electron binding energies are sufficiently small to be neglected.

In this work, ^{25}Mg (m = 24.98583698(5) u [32]) and ^{30}Si (m = 29.973770136(23) u [32]) were used as references for ^{25}Al and ^{30}P, respectively. Both reference ions were directly produced from the Si and ZnS targets. The use of ^{25}Mg and ^{30}Si as references had the benefit that systematic effects resulting from field imperfections cancel in the frequency ratio [33]. However, the uncertainty due to temporal fluctuations of the magnetic field strength has to be taken into account for the measured frequency ratios. Since JYFLTRAP was moved to IGISOL-4, the 7-T superconducting solenoid housing it had to be re-energized. To quantify the present magnitude of temporal fluctuations in the magnetic field strength, a separate experiment was carried out in December 2014.

The temporal fluctuations of the magnetic field were studied by measuring the cyclotron frequency of ^{84}Kr^{+} ions for one week with a Ramsey excitation pattern of 25 ms (On)-350 ms (Off)-25 ms (On) with an amplitude of 224 mV. The fluctuation was determined by comparing the cyclotron frequency obtained via interpolating from two reference measurements separated by time Δt to the cyclotron frequency measured in the middle of these two reference measurements. The data were split into ≈9.5-min-long measurements, thus the shortest time difference between the references was ≈19 min. Standard deviations from the weighted average of the frequency ratio were computed for each possible Δt and plotted as a function of Δt (see Fig. 2). The obtained magnetic field fluctuation as a function of time is $\sigma_B(\nu_{c,ref})/\nu_{c,ref} = 8.18(19) \times 10^{-12}/\text{min}\times\Delta t$ which is less than previously measured at IGISOL-3, $3.22(16) \times 10^{-11}/\text{min}\times\Delta t$ [34] and $5.7(8) \times 10^{-11}/\text{min}\times\Delta t$ [35]. This is likely to be due to smaller temperature variations at IGISOL-4. Daily fluctuations of temperature were below 0.6°C in the laboratory. The facility is now located in a separate hall without direct access to outdoors and insulators have been added to the high-voltage cage of JYFLTRAP resulting in more stable conditions. Also, the magnet stand is now made of aluminium and thus does not contain ferromagnetic material anymore.

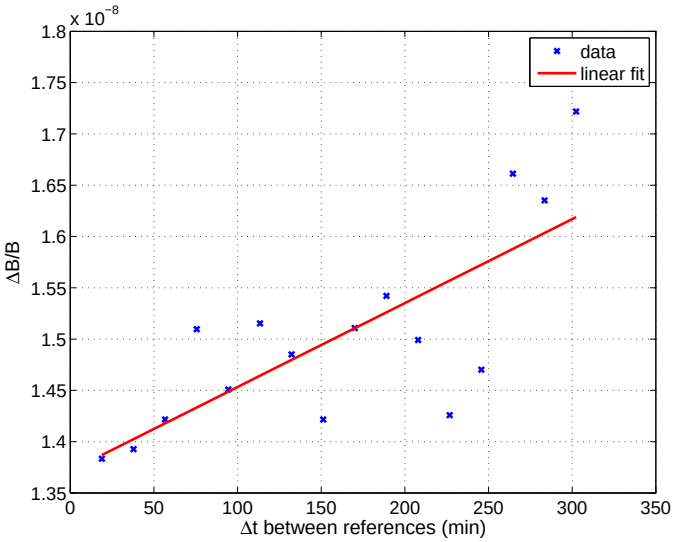

Fig. 2. Standard deviation of the magnetic field obtained for different time differences Δt between two reference measurements taken during one week of frequency measurements using a Ramsey excitation pattern of 25 ms (On)-350 ms (Off)-25 ms (On). The slope of the fit is $8.18(19) \times 10^{-12}$/min.

Table 1. Number of measurements #, frequency ratios r and the mass-excess Δ, Q_{EC} and $Q_{(p,\gamma)}$ values (in keV) determined in this work in comparison with the AME12 values. ^{25}Mg^{+} ions were used as a reference for ^{25}Al and ^{30}Si^{+} for ^{30}P.

Ion	^{25}Al	^{30}P
#	42	12
r	1.0001837618(19)	1.0001515804(22)
Δ	-8915.962(63)	-20200.854(64)
Δ_{AME12}	-8916.2(5)	-20200.6(3)
Difference	0.2(5)	-0.2(3)
Q_{EC}	4276.805(45)	4232.106(60)
$Q_{EC,AME12}$	4276.6(5)	4232.4(3)
$Q_{(p,\gamma)}$	5513.99(13)	6130.64(24)
$Q_{(p,\gamma),AME12}$	5513.8(5)	6130.9(4)

3 Results

3.1 The results for ^{25}Al

The results of this work are summarized in Table 1. In total, 42 frequency ratios were measured within 20 hours for ^{25}Al. The weighted mean of the frequency ratios gives r = 1.0001837618(19) (see Fig. 3). The Birge ratio was 0.98 [36] which shows that there are not hidden systematic errors in our data. Therefore, the inner error was taken as the final uncertainty.

The measured mass excess value for ^{25}Al, −8915.962(63) keV, is very close to, but about 7 times more precise than the adopted value in the AME12 [32]. The AME12 value is based on ^{25}Mg$(p,n)^{25}$Al [37] and ^{24}Mg$(p,\gamma)^{25}$Al [38–40] experiments (see Fig. 4). With our new direct mass measurement of ^{25}Al we can confirm the adopted value and improve the accuracy of the ^{25}Al mass considerably.

We also directly measured the Q_{EC} value of ^{25}Al which is important for fundamental physics as it is an isospin T = 1/2 mirror nucleus. Mirror beta decay Q_{EC} values can be used to extract data for testing the Conserved Vector Current hypothesis provided that the Fermi to Gamow-Teller mixing ratio is already known [41,42]. In this work, we have improved the precision from 500 eV to 45 eV. A more precise Q$_{EC}$ value will result in a more precise ft value for the beta decay which can be used to determine *e.g.* the mixing ratio.

Since the mass of ^{26}Si has already been precisely measured with JYFLTRAP [13], a precise proton-capture Q value for ^{25}Al$(p,\gamma)^{26}$Si, $Q_{(p,\gamma)}$ = 5513.99(13) keV, is obtained with the new ^{25}Al mass-excess value. The impact of the new Q value on the astrophysical resonant capture calculations is discussed in section 4.

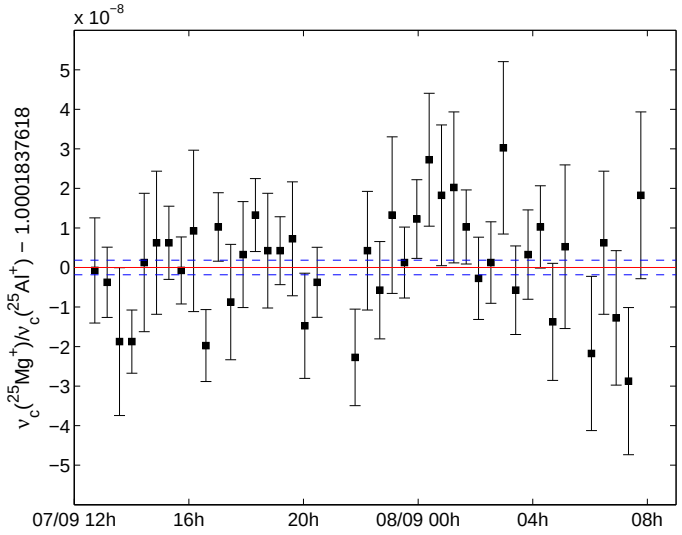

Fig. 3. Measured frequency ratios for ^{25}Al. The red line corresponds to the weighted mean of the frequency ratios and the dashed lines show the 1σ uncertainty limits.

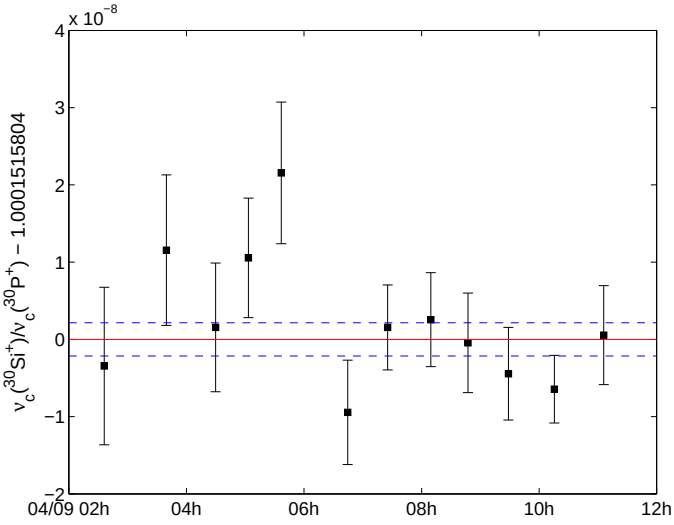

Fig. 5. Measured frequency ratios for ^{30}P. The red line corresponds to the weighted mean of the frequency ratios and the dashed lines show the 1σ uncertainty limits.

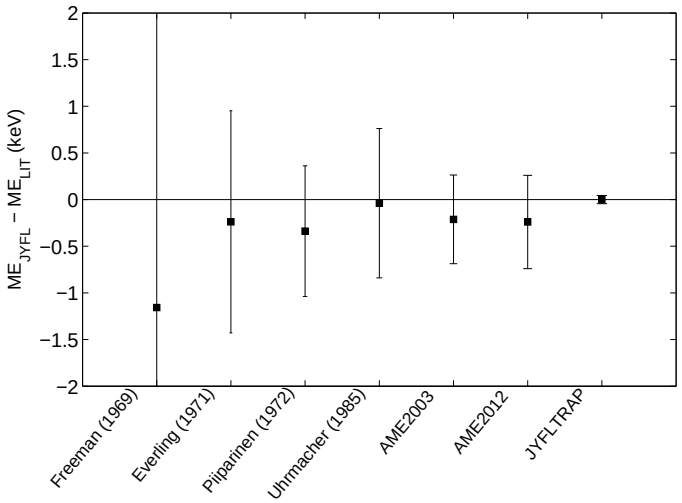

Fig. 4. Mass-excess values of ^{25}Al from previous experiments in comparison with the new JYFLTRAP value. From left to right: Freeman *et al.* ^{25}Mg$(p,n)^{25}$Al [37], Everling *et al.* ^{24}Mg$(p,\gamma)^{25}$Al [38], Piiparinen ^{24}Mg$(p,\gamma)^{25}$Al [39], Uhrmacher *et al.* ^{24}Mg$(p,\gamma)^{25}$Al [40], AME03 [43] and AME12 [32]

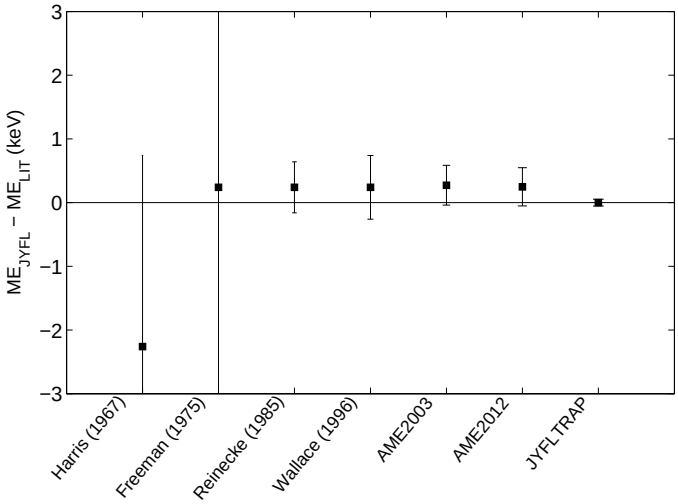

Fig. 6. Mass-excess values of ^{30}P from previous experiments in comparison with the new JYFLTRAP value. From left to right: Harris *et al.* ^{29}Si$(p,\gamma)^{30}$P [44], Freeman *et al.* ^{30}Si$(p,n)^{30}$P [47], Reinecke *et al.* ^{29}Si$(p,\gamma)^{30}$P [45], Wallace *et al.* ^{29}Si$(p,\gamma)^{30}$P [46], AME03 [43] and AME12 [32].

3.2 The results for ^{30}P

Altogether twelve frequency ratios were measured for ^{30}P (see Fig. 5). The Birge ratio was 1.13, and thus the outer error was adopted as the final error of the weighted mean $r = 1.0001515804(22)$. The obtained mass-excess value for ^{30}P, -20200.854 (64) keV, is a little lower than in AME12 but almost five times more precise. The adopted mass value of ^{30}P in AME12 has been mainly based on ^{29}Si$(p,\gamma)^{30}$P [44–46] and ^{30}Si$(p,n)^{30}$P [47] measurements (see Fig. 6). Our new Penning-trap measurement is in a good agreement with the earlier experiments.

The proton-capture Q value for the ^{30}P$(p,\gamma)^{31}$S reaction, $Q_{(p,\gamma)} = 6130.64(24)$ keV, has been determined with an improved precision using the AME12 mass for ^{31}S based on a previous JYFLTRAP measurement [18] and the newly measured ^{30}P mass. The impact of the new proton-capture Q value on resonant proton-capture rates is discussed in section 4.

4 Discussion

In this section we discuss the impact of the new $Q_{(p,\gamma)}$ values on the resonant proton-capture rates on ^{25}Al and

^{30}P. For both nuclei, the proton captures are dominated by resonant captures to a few states above the proton threshold in ^{26}Si and ^{31}S, respectively. In general, the total resonant proton capture rate $N_A \langle \sigma v \rangle_{res}$ can be summed over individual resonances to resonance states i located at excitation energies $E_{x,i}$ with resonance energies $E_{r,i} = E_{x,i} - Q_{(p,\gamma)}$:

$$N_A \langle \sigma v \rangle_{res} = 1.54 \times 10^{11} (\mu T_9)^{-3/2} \sum_i (\omega\gamma)_i \times \exp(-11.605 E_{r,i}/T_9) \text{ cm}^3\text{mol}^{-1}\text{s}^{-1} , \quad (4)$$

where the resonance energies are given in MeV, μ is the reduced mass in atomic mass units, T_9 temperature in GK and $\omega\gamma_i$ is the resonance strength. The resonance strength $\omega\gamma_i$ for an isolated resonance in a (p,γ) reaction is given by:

$$\omega\gamma = \frac{2J_i + 1}{2(2J_t + 1)} \frac{\Gamma_p \Gamma_\gamma}{\Gamma_{\text{tot}}}, \quad (5)$$

where J_i and J_t are the spins of the resonance state and the target nucleus ($J_t = 5/2$ for ^{25}Al and $J_t = 1$ for ^{30}P) and the total width Γ_{tot} is the sum of the proton width Γ_p and the gamma width Γ_γ. The proton widths have been scaled from the literature values using the relation [48]:

$$\Gamma_p \propto \exp\left(-31.29 Z_1 Z_2 \sqrt{\frac{\mu}{E_r}}\right), \quad (6)$$

where Z_1 and Z_2 are the proton numbers of the incoming particles, μ is the reduced mass in u and E_r is the center-of-mass resonance energy in keV [48].

The new proton-capture Q value for ^{25}Al$(p,\gamma)^{26}$Si is 5513.99(13) keV, which is 0.2 keV higher than in AME12 ($Q_{(p,\gamma)}$ = 5513.8(5) keV [32]) and around 3 keV lower than in AME03 ($Q_{(p,\gamma)}$ = 5517(3) keV [43]). Although the Q value did not change dramatically, the uncertainties related to the proton-capture Q value have been reduced considerably with the high-precision measurements of ^{25}Al (this work) and ^{26}Si [13] at JYFLTRAP: the Q value is now 23 times and 4 times more precise than in AME03 and AME12 respectively.

The resonant proton captures on ^{25}Al are dominated by captures to a few levels with rather low resonance energies. The knowledge of these states has improved considerably thanks to several measurements on the excited levels of ^{26}Si [49–61]. Gamma-decay studies of ^{26}Si performed at Gammasphere [54,60] have shown that there is a 4^+ state at 5517.0 keV, a 1^+ level at 5675.9 keV and a 0^+ state at 5890.1 keV. A 3^+ state at 5928.7 keV has been confirmed via beta-decay studies of ^{26}P [51,58] and it is also supported by [50,53,56]. The spin for the next excited state at 5946 keV is unclear. It has been claimed to be a 0^+ [52] as well as 3^+ [49]. The shell-model calculations [62] suggest it to be 0^+ but interestingly, they do not predict another 0^+ state at around 5890 keV although it has been experimentally observed [57,59,60]. The resonant proton captures to the 1^+ state at 5676 keV dominate the total reaction rate at temperatures below $T \approx 0.15$ GK. At higher temperatures, the captures to the 3^+ state take over (see Fig. 7.(a)).

To demonstrate the effect of the JYFLTRAP $Q_{(p,\gamma)}$ value for the ^{25}Al$(p,\gamma)^{26}$Si reaction, we have calculated the resonant proton-capture rates in ^{26}Si using the $Q_{(p,\gamma)}$ values from AME03 [43], AME12 [32] and from this work (see Fig. 7) to the dominating 1^+, 0^+ and 3^+ states. The level at 5946 keV was not included due to its uncertain spin and parity assignments. The corresponding excitation energies 5675.9(11) keV, 5890.1(6) keV and 5928.7(7) keV were taken from Doherty *et al.* [60] for the 1^+ and 0^+ states, and from Bennett *et al.* [58] for the 3^+ state. We also calculated upper and lower limits for the rates by taking into account the uncertainties in the Q values and compared the widths of these uncertainty bands to each other. For calculating the resonance strengths, proton widths from Ref. [62] for the 1^+ state, $\Gamma_p = 6.30 \times 10^{-9}$ eV (E_{res} = 163 keV), the 0^+ state $\Gamma_p = 1.6 \times 10^{-2}$ eV (E_{res} = 434 keV) and the 3^+ state $\Gamma_p = 3.5$ eV (E_{res} = 403 keV) have been scaled using Eq. 6. A gamma width of $\Gamma_\gamma = 0.12$ eV was used for the 1^+ and 3^+ states and $\Gamma_\gamma = 8.8 \times 10^{-3}$ eV for the 0^+ state similar to Ref. [62]. As can be seen from Fig. 7.(b), the JYFLTRAP and AME12 rates are very close to each other: the JYFLTRAP Q value gives a few percent higher capture rate than the AME12 value. The Q-value-related uncertainties have been reduced by around 10-15 % compared to the AME12 value and 60-80 % compared to the AME03 value (see Fig. 7.(c)).

The proton-capture Q value obtained for ^{30}P$(p,\gamma)^{31}$S in this work, 6130.64(24) keV, is ≈0.2 keV lower than in AME12 ($Q_{(p,\gamma)}$ = 6130.9(4) keV [32]) and 2.4 keV lower than in AME03 ($Q_{(p,\gamma)}$ = 6133.0(15) keV [43]). The $Q_{(p,\gamma)}$ value is now known with an ≈6 times better precision than in AME03 and almost 2 times better than in AME12 due to the JYFLTRAP measurements of ^{30}P (this work) and ^{31}S [18]. The impact of the new Q value on the resonant proton-capture rate on ^{30}P was studied similarly to the ^{25}Al$(p,\gamma)^{26}$Si reaction. There are more known resonant states above the proton separation energy in ^{31}S than in ^{26}Si, and they are rather well-known via studies at Gammasphere employing both heavy-ion fusion-evaporation reactions [63,64], and more recently, light-ion fusion-evaporation reactions [65,66]. The resonance states have also been explored *e.g.* via ^{31}P$(^3\text{He},t)^{31}$S reactions at Yale University's Wright Nuclear Structure Laboratory [67,68] and at Maier-Leibnitz-Laboratorium in Garching [69]. A recent review [70] gives a thorough summary of the previous studies and relevant states in ^{31}S.

Here, we have calculated the resonant proton-capture rates to the $1/2^+$ (E_{res} = 128.4 keV), $3/2^-$ (E_{res} = 196.4 keV), $5/2^-$ (E_{res} = 226.7 keV), $9/2^-$ (E_{res} = 246.3 keV), $5/2^+$ (E_{res} = 261.9 keV), $11/2^+$ (E_{res} = 263.6 keV), $3/2^-$ (E_{res} = 411.3 keV) and $7/2^-$ (E_{res} = 452.5 keV) states to demonstrate the effect of the new Q value (see Fig. 8). The resonant proton captures on ^{30}P are dominated by captures to the $1/2^+$ (E_{res} = 128.4 keV) state below $T \approx 0.08$ GK and to the $3/2^-$ (E_{res} = 196.4 keV) state at $T \approx 0.08 - 0.2$ GK. At around $T = 0.2$ GK, captures to the $11/2^+$ (E_{res} = 263.6 keV) state become important,

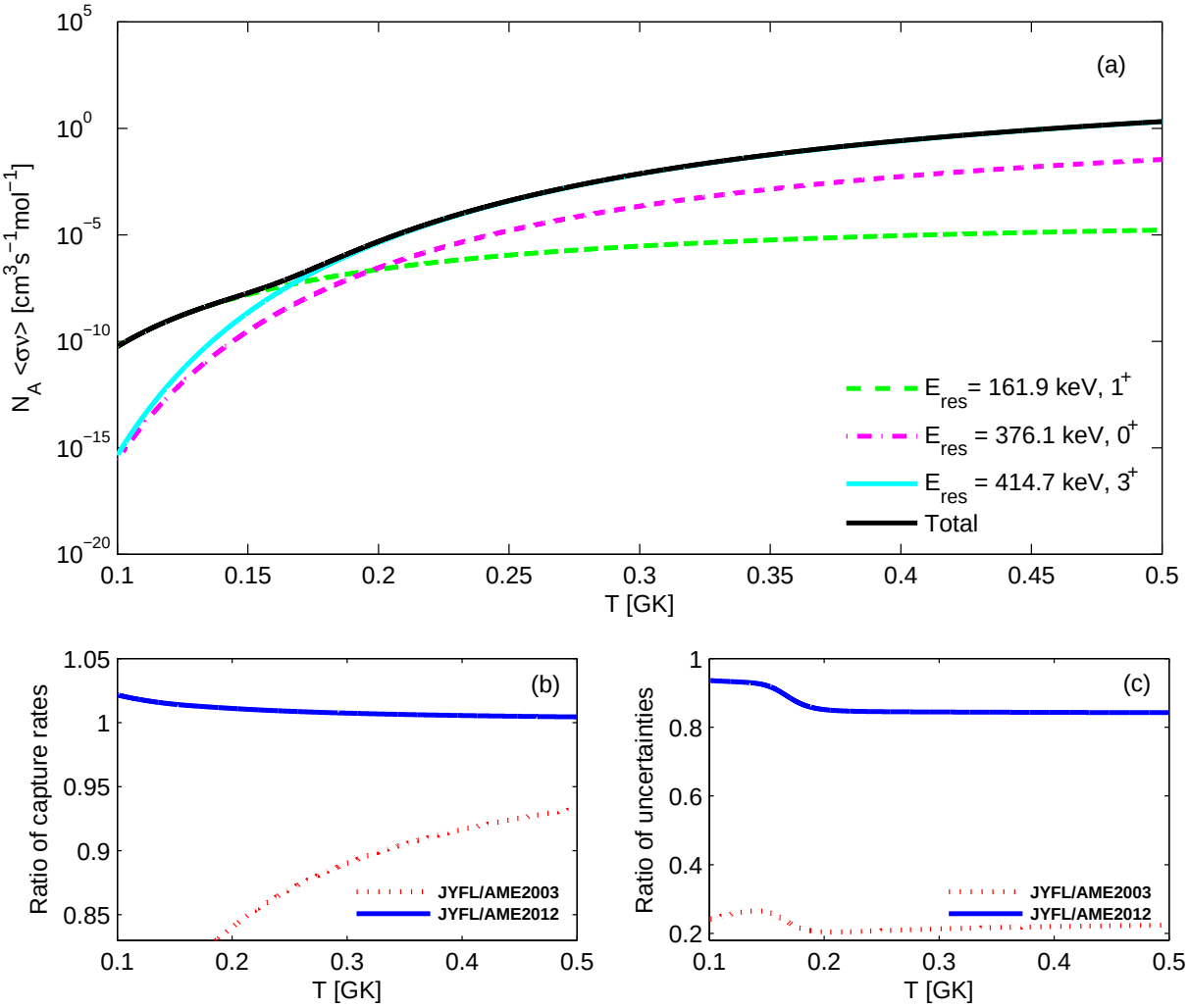

Fig. 7. (a) The resonant proton-capture rates to the 1^+, 0^+ and 3^+ states in ^{26}Si calculated with the $Q_{(p,\gamma)}$ value from this work (JYFL). (b) Ratios of the total resonant proton-capture rate calculated with the JYFLTRAP $Q_{(p,\gamma)}$ value and with the values from AME03 [43] or AME12 [32]. (c) Ratios of the Q-value-related uncertainties in the calculated total resonant proton-capture reaction rates.

and at higher temperatures, the $3/2^-$ ($E_{res} = 411.3$ keV) and $7/2^-$ ($E_{res} = 452.5$ keV) states dominate. The proton widths have been scaled from Ref. [67] using Eq. 6 and the excitation energies were taken from [65,70]. The state at 6357 keV ($E_{res} = 226.7$ keV) has contradictory spin assignments of $3/2^+$ [69], $5/2^+$ [67,68], and $5/2^-$ [65,66]. Here we have adopted the same assignment as in Ref. [67, 68] but note that this choice may have an effect on the reaction rate at lower temperatures. The revised total resonant proton capture rate is very close to the result obtained with the AME12 value (see Fig. 8.(b)) and the mass-related uncertainties have been reduced by 5-20 % compared to the AME12 and 40-70 % compared to the AME03 (see Fig. 8.(c)).

5 Conclusions

We have performed the first Penning-trap mass measurements of ^{25}Al and ^{30}P at JYFLTRAP resulting in an unparalleled precision of respectively 63 eV and 64 eV in the mass-excess values. Our results agree with the adopted values in AME12 [32] which are mainly based on (p,γ) reaction studies, and thus confirm that those experiments have not suffered from significant systematic uncertainties. The experiment was also the first on-line mass measurement of neutron-deficient nuclei at IGISOL-4, and therefore an additional study of the stability of the magnetic field inside the JYFLTRAP was carried out using ^{84}Kr$^+$ ions. The temporal fluctuations in the magnetic field were found to be smaller than at the old IGISOL-3 facility, likely to be due to better temperature regulation in the new laboratory hall. The effect of new, more precise mass values on calculated resonant proton capture rates on ^{25}Al and ^{30}P have been studied. These reactions, ^{25}Al$(p,\gamma)^{26}$Si

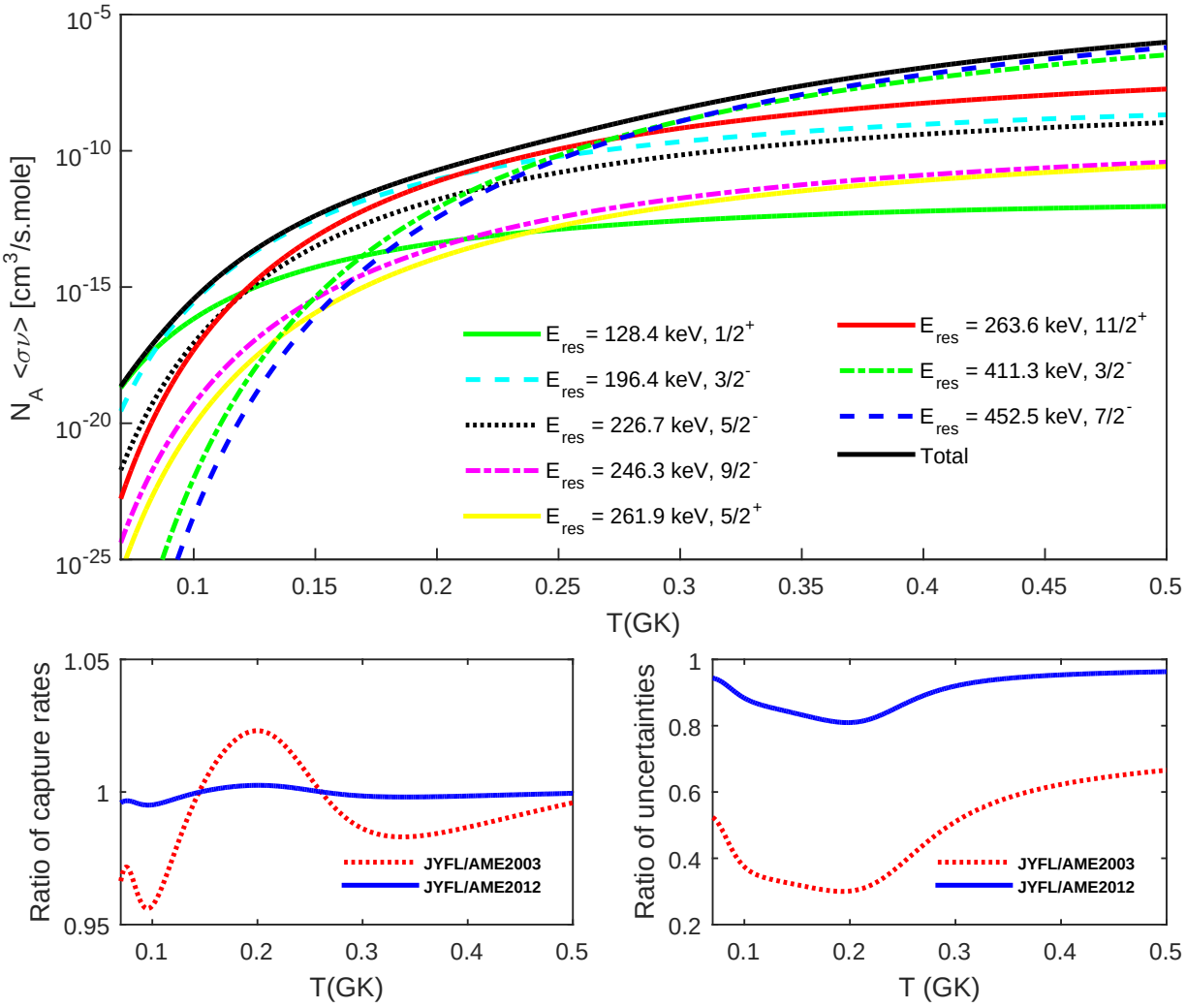

Fig. 8. (a) The resonant proton-capture rates to the $1/2^+$,$3/2^-$, $5/2^-$, $9/2^-$, $5/2^+$, $11/2^+$, $3/2^-$ and $7/2^-$ states in ^{31}S calculated with the $Q_{(p,\gamma)}$ value from this work (JYFL). (b) Ratios of the total resonant proton-capture rate calculated with the JYFLTRAP $Q_{(p,\gamma)}$ value and the values from AME03 [43] or AME12 [32]. (c) Ratios of the Q-value-related uncertainties in the calculated total resonant proton-capture reaction rates.

and ^{30}P$(p,\gamma)^{31}$S, are crucial for estimating the production of ^{26}Al in Galaxy and the abundancies of elements heavier than sulphur synthesized in novae. Although the JYFLTRAP Q values did not change the calculated resonant capture rates considerably, the more accurate Q values reduce the mass-related uncertainties in the reaction rates by ≈15 % compared to the AME12 values, and confirm that there are no systematic uncertainties related to the adopted Q values.

6 Acknowledgements

This work has been supported by the EU 7th framework programme Integrating Activities - Transnational Access, project number: 262010 (ENSAR) and by the Academy of Finland under the Finnish Centre of Excellence Programme 2012-2017 (Nuclear and Accelerator Based Physics Research at JYFL). A.K. and L.C. acknowledge the support from the Academy of Finland under project No. 275389.

References

1. J. S. Gallagher, and S. Starrfield, Ann. Rev. Astron. Astrophys. **16**, 171-214 (1978).
2. A. Parikh, J. José, and G. Sala, AIP Advances **4**, 041002 (2014).
3. J. José, M. Hernanz, and C. Iliadis, Nucl. Phys. A **777**, 550 (2006), special Issue on Nuclear Astrophysics.
4. J. José and M. Hernanz, J. Phys. G: Nucl. and Part. Phys. **34**, R431 (2007).
5. J. José and C. Iliadis, Rep. Progr. in Phys. **74**, 096901 (2011).
6. J. José, M. Hernanz, and A. Coc, Astrophys. J. Lett. **479**, L55 (1997).

7. J. José, A. Coc, and M. Hernanz, Astrophys. J. **520**, 347 (1999).
8. W. A. Mahoney, J. C. Ling, A. S. Jacobson, and R. E. Lingenfelter, Astrophys. J. **262**, 742 (1982).
9. R. Diehl *et al.*, Astron. Astrophys. **298**, 445 (1995).
10. R. Diehl *et al.*, Nature **439**, 45 (2006).
11. R. Diehl, Astron. Rev. **8**, 030000 (2013).
12. R. Diehl, Rep. Progr. Phys. **76**, 026301 (2013).
13. T. Eronen *et al.*, Phys. Rev. C **79**, 032802 (2009).
14. J. José and M. Hernanz, Astrophys. J. **494**, 680 (1998).
15. J. José, A. Coc, and M. Hernanz, Astrophys. J. **560**, 897 (2001).
16. S. Amari *et al.*, Astrophys. J. **551**, 1065 (2001).
17. J. José *et al.*, Astrophys. J. **612**, 414 (2004).
18. A. Kankainen *et al.*, Phys. Rev. C **82**, 052501 (2010).
19. G. Audi *et al.*, Chin. Phys. C **36**, 1287 (2012).
20. I. Moore *et al.*, Nucl. Instrum. and Methods in Phys. Res. B **317, Part B**, 208 (2013).
21. V. Kolhinen *et al.*, Nucl. Instrum. and Methods in Phys. Res. B **317, Part B**, 506 (2013).
22. T. Eronen *et al.*, Eur. Phys. J. A **48**, 46 (2012).
23. P. Karvonen *et al.*, Nucl. Instrum. and Methods in Phys. Res. B **266**, 4794 (2008).
24. A. Nieminen *et al.*, Nucl. Instrum. and Methods in Phys. Res. A **469**, 244 (2001).
25. G. Savard *et al.*, Phys. Lett. A **158**, 247 (1991).
26. M. König *et al.*, Int. J. Mass Spectrom. and Ion Processes **142**, 95 (1995).
27. G. Gräff, H. Kalinowsky, and J. Traut, Z. Phys. A **297**, 35 (1980).
28. S. George *et al.*, Int. J. Mass Spectrom. **264**, 110 (2007).
29. S. George *et al.*, Phys. Rev. Lett. **98**, 162501 (2007).
30. M. Kretzschmar, Int. J. Mass Spectrom. **264**, 122 (2007).
31. A. Kellerbauer *et al.*, Eur. Phys. J. D **22**, 53 (2003).
32. M. Wang *et al.*, Chin. Phys. C **36**, 1603 (2012).
33. C. Roux *et al.*, Eur. Phys. J. D **67**, (2013).
34. S. Rahaman *et al.*, Eur. Phys. J. A **34**, 5 (2007).
35. V.-V. Elomaa *et al.*, Nucl. Instrum. and Methods in Phys. Res. A **612**, 97 (2009).
36. R. T. Birge, Phys. Rev. **40**, 207 (1932).
37. J. M. Freeman *et al.*, Nucl. Phys. A **132**, 593 (1969).
38. F. Everling *et al.*, Can. J. Phys. **49**, 402 (1971).
39. M. Piiparinen, Z. Phys. **252**, 206 (1972).
40. M. Uhrmacher *et al.*, Nucl. Instrum. and Methods in Phys. Res. B **9**, 234 (1985).
41. N. Severijns, M. Tandecki, T. Phalet, and I. S. Towner, Phys. Rev. C **78**, 055501 (2008).
42. O. Naviliat-Cuncic and N. Severijns, Phys. Rev. Lett. **102**, 142302 (2009).
43. G. Audi, A. Wapstra, and C. Thibault, Nucl. Phys. A **729**, 337 (2003).
44. G. I. Harris and A. K. Hyder, Phys. Rev. **157**, 958 (1967).
45. J. Reinecke *et al.*, Nucl. Phys. A **435**, 333 (1985).
46. P. M. Wallace *et al.*, Phys. Rev. C **54**, 2916 (1996).
47. J.M.Freeman *et al.*, *Proceedings of 5th Int. Conf. Atomic Masses and Fundamental constants AMCO-5, p. 126*, 1975.
48. C. E. Rolfs and W. S. Rodney, *Cauldrons in the Cosmos* (The University Chicago Press, Chicago, 1988).
49. J. A. Caggiano *et al.*, Phys. Rev. C **65**, 055801 (2002).
50. D. W. Bardayan *et al.*, Phys. Rev. C **65**, 032801 (2002).
51. J.-C. Thomas *et al.*, Eur. Phys. J. A **21**, 419 (2004).
52. Y. Parpottas *et al.*, Phys. Rev. C **70**, 065805 (2004).
53. D. W. Bardayan *et al.*, Phys. Rev. C **74**, 045804 (2006).
54. D. Seweryniak *et al.*, Phys. Rev. C **75**, 062801 (2007).
55. P. N. Peplowski *et al.*, Phys. Rev. C **79**, 032801 (2009).
56. K. A. Chipps *et al.*, Phys. Rev. C **82**, 045803 (2010).
57. N. de Séréville *et al.*, PoS **NIC XI**, 212 (2010).
58. M. B. Bennett *et al.*, Phys. Rev. Lett. **111**, 232503 (2013).
59. T. Komatsubara *et al.*, Eur. Phys. J. A **50**, (2014).
60. D. T. Doherty *et al.*, Phys. Rev. C **92**, 035808 (2015).
61. Y. Parpottas *et al.*, Phys. Rev. C **73**, 049907 (2006).
62. W. A. Richter, B. A. Brown, A. Signoracci, and M. Wiescher, Phys. Rev. C **83**, 065803 (2011).
63. D. G. Jenkins *et al.*, Phys. Rev. C **72**, 031303 (2005).
64. D. G. Jenkins *et al.*, Phys. Rev. C **73**, 065802 (2006).
65. D. T. Doherty *et al.*, Phys. Rev. Lett. **108**, 262502 (2012).
66. D. T. Doherty *et al.*, Phys. Rev. C **89**, 045804 (2014).
67. C. Wrede *et al.*, Phys. Rev. C **76**, 052802 (2007).
68. C. Wrede *et al.*, Phys. Rev. C **79**, 045803 (2009).
69. A. Parikh *et al.*, Phys. Rev. C **83**, 045806 (2011).
70. C. Wrede, AIP Advances **4**, 041004 (2014).